Mass and heat fluxes for a binary granular mixture at low density

Vicente Garzó[a)]
Departamento de Física, Universidad de Extremadura, E-06071 Badajoz, Spain

José María Montanero[b)]
Departamento de Electrónica e Ingeniería Electromecánica, Universidad de Extremadura, E-06071 Badajoz, Spain

James W. Dufty[c)]
Department of Physics, University of Florida, Gainesville, Florida 32611

(Received 11 February 2006; accepted 13 July 2006; published online 31 August 2006)

The Navier–Stokes order hydrodynamic equations for a low-density granular mixture obtained previously from the Chapman–Enskog solution to the Boltzmann equation are considered further. The six transport coefficients associated with mass and heat flux in a binary mixture are given as functions of the mass ratio, size ratio, composition, and coefficients of restitution. Their quantitative variation across this parameter set is demonstrated using low-order Sonine polynomial approximations to solve the exact integral equations. The results are also used to quantify the violation of the Onsager reciprocal relations for a granular mixture. Finally, the stability of the homogeneous cooling state is discussed. © *2006 American Institute of Physics*.
[DOI: 10.1063/1.2336755]

I. INTRODUCTION

The relevance and context of a hydrodynamic description for granular gases remain a controversial topic. At sufficiently low density the origin of hydrodynamics can be studied from Boltzmann kinetic theory.[1,2] To obtain hydrodynamics from the Boltzmann kinetic equation the essential assumption is the existence of a "normal" solution, defined to be one for which all space and time dependence occurs through the macroscopic hydrodynamic fields.[3] This solution, together with the macroscopic balance equations, leads to a closed set of hydrodynamic equations for these fields. The Chapman–Enskog method provides a constructive means to obtain an approximation to such a solution for states whose spatial gradients are not too large. In this general context, the study of hydrodynamics for granular gases is the same as that for normal gases.

The details of the Chapman–Enskog method have been carried out for a granular one-component gas to obtain the Navier–Stokes order hydrodynamic equations, together with exact integral equations determining the transport coefficients occurring in these equations.[4] These integral equations have been solved approximately using Sonine polynomial expansions and compared to both direct simulation Monte Carlo (DSMC) of the Boltzmann equation and molecular dynamics (MD) simulation of the gas.[5] Good agreement is obtained even for relatively strong degrees of dissipation. The results support the formal theoretical analysis and the claim that hydrodynamics is not limited to the quasielastic limit.

The analysis for multicomponent granular gases is much more complicated than for a one-component gas. Most of the previous attempts[6] were made for *nearly* elastic spheres, where the equipartition of energy can be considered as an acceptable assumption. In addition, according to this level of approximation, the inelasticity is only accounted for by the presence of a sink term in the energy balance equation, so that the expressions for the transport coefficients are the same as those obtained for normal fluids.[7] However, the theoretical prediction of the failure of energy equipartition in multicomponent granular gases[8] also has been confirmed by computer simulations,[9] and even observed in real experiments.[10] Although the possibility of nonequipartition was already pointed out many years ago,[11] it has not been until recently that a systematic study of the effect of nonequipartition on transport has been carefully analyzed. In this context, Garzó and Dufty[12] have carried out a derivation of the Navier–Stokes hydrodynamic equations for a binary mixture at low density that accounts for nonequipartition of granular energy. These equations and associated transport coefficients provide a somewhat more stringent test of the analysis since the parameter space is much larger. There are now many more transport coefficients, given as functions of the three independent coefficients of restitution, size ratio, mass ratio, and composition. As in the one-component case, explicit expressions for the transport coefficients requires also to consider Sonine polynomial expansions. The numerical accuracy of this Sonine expansion has been confirmed by comparison with Monte Carlo simulations of the Boltzmann equation in the cases of the shear viscosity[13] and the tracer diffusion[14] coefficients. Exceptions to this agreement are extreme mass or size ratios and strong dissipation, although these discrepancies between theory and simulation diminish as one considers more terms in the Sonine polynomial approximation.[14]

Since the dependence of the shear viscosity coefficient

[a)]Electronic mail: vicenteg@unex.es
[b)]Electronic mail: jmm@unex.es
[c)]Electronic mail: dufty@phys.ufl.edu

on the parameters of the mixture (masses, sizes, concentration, coefficients of restitution) has been widely studied in a previous work,[13] a primary objective here is to demonstrate the variation of the six transport coefficients associated with the mass and heat flux in this parameter space, using the same Sonine polynomial approximation as was found applicable for the one-component gas. To set the context for these quantitative results three qualitative and potentially confusing issues are briefly noted at the outset.

There is some ambiguity regarding the hydrodynamic temperature in a mixture since temperatures for each species can be defined in addition to the global temperature. What should be the hydrodynamic fields? For normal gases the answer is clear. These are set by the slow variables (at large space and time scales) associated with conserved quantities. In addition to species number and total momentum, only the total kinetic energy is conserved, so only one global temperature occurs as an additional hydrodynamic field. The energy is no longer conserved for granular gases, but it remains a slow variable if the cooling rate is not too large. This is confirmed by noting that Haff's cooling law is the hydrodynamic mode at long wavelengths, and MD simulation confirms that this dominates after a transient period of a few collision times.[15] Thus, in this case as well, only the global temperature should appear among the hydrodynamic fields.

Nevertheless, the species temperatures play a new and interesting secondary role. For a normal (molecular) gas, there is a rapid velocity relaxation in each fluid cell to a local equilibrium state on the time scale of a few collisions (e.g., as illustrated by the approach to Haff's law). Subsequently, the equilibration among cells occurs via the hydrodynamic equations. In each cell the species velocity distributions are characterized by the species temperatures. These are approximately the same due to equipartition, and the hydrodynamic relaxation occurs for the single common temperature.[3] A similar rapid velocity relaxation occurs for granular gases in each small cell, but to a universal state different from local equilibrium and one for which equipartition no longer occurs. Hence, the species temperatures T_i are different from each other and from the overall temperature T of the cell. Nevertheless, the time dependence of all temperatures is the same in this and subsequent states, i.e., they are proportional to the global temperature $T_i(t)=\gamma_i T(t)$ (Ref. 8). This implies that the species temperatures do not provide any new dynamical degree of freedom at the hydrodynamic stage. However, they still characterize the shape of the partial velocity distributions and affect the quantitative averages calculated with these distributions. The transport coefficients for granular mixtures therefore have new quantitative effects arising from the time-independent temperature ratio γ_i for each species.[12] This dependence is illustrated here as well.

In some earlier works,[11,16] additional equations for each species temperature have been included among the hydrodynamic set. This is possible since the overall temperature is determined from these by $T(t)=\Sigma_i x_i T_i(t)$, where x_i is the concentration of species i. However, this is an unnecessary complication, describing additional kinetics beyond hydrodynamics that is relevant only on the time scale of a few collisions. As described above (and supported by molecular-dynamics simulations[15]) the dynamics of all species temperatures quickly reduces to that of $T(t)$. The remaining time-independent determination of the γ_i follows directly from the condition that the cooling rates of all temperatures be the same.

A second confusing issue is the context of the Navier–Stokes equations considered here. The derivation of the Navier–Stokes order transport coefficients does not limit their application to weak inelasticity. For this reason the results reported below include a domain of both weak and strong inelasticity, $0.5\leq\alpha\leq 1$. The Navier–Stokes hydrodynamic equations themselves may or may not be limited with respect to inelasticity, depending on the particular states considered. The derivation of these equations by the Chapman–Enskog method assumes that relative changes in the hydrodynamic fields over distances of the order of a mean free path are small. For normal gases this can be controlled by the initial or boundary conditions. It is more complicated for granular gases. In some cases (e.g., steady states such as the simple shear flow problem[17]) the boundary conditions imply a relationship between the coefficient of restitution and some hydrodynamic gradient—the two cannot be chosen independently. Consequently, there are examples for which the Navier–Stokes approximation is never valid or is restricted to the quasielastic limit.[17] However, the transport coefficients characterizing the Navier–Stokes order hydrodynamic equations are well-defined functions of α, regardless of the applicability of those equations [e.g., the coefficients of a Taylor series for some function $f(\alpha,x)$ in powers of x may be defined for all α at each order, even when the series cannot be truncated at that order].

In spite of the above cautions, the Navier–Stokes approximation is appropriate and accurate for a wide class of flows. One group refers to spatial perturbations of the homogeneous cooling state (HCS) for an isolated system. Both MD and DSMC simulations[5] have confirmed the dependence of the Navier–Stokes transport coefficients on the coefficient of restitution, and application of the Navier–Stokes hydrodynamics with these coefficients to describe cluster formation has been also confirmed quantitatively (e.g., see Ref. 18). The same kinetic theory results apply to driven systems as well. This is so since the reference state is a *local* HCS whose parameters vary throughout the system to match the physical values in each cell. Examples include application of Navier–Stokes hydrodynamics from kinetic theory to symmetry breaking and density/temperature profiles in vertical vibrated gases, for comparison with simulation.[19] Similar comparison with Navier–Stokes hydrodynamics of the latter and of supersonic flow past a wedge in real experiments has been given,[20,21] showing both qualitative and quantitative agreement. In summary, the Navier–Stokes equations with the constitutive equations derived here remain an important and useful description for a wide class of granular flow, although more limited than for normal gases.

The plan of the paper is as follows. First, in Sec. II the hydrodynamic equations and associated fluxes to Navier–Stokes order are recalled, and the expressions for the transport coefficients for heat and mass transport are given to leading Sonine polynomial approximation. The elastic limit

is discussed to aid in the interpretation of these expressions. Next, in Sec. III the results for these six coefficients are illustrated for a common coefficient of restitution α and same size ratio as functions of α at a composition $x_1=0.2$ for several values of the mass ratio. With the exception of thermal conductivity, the deviations from normal gas values are largest at small α and large mass ratio. The usual Onsager relations among these coefficients for normal gases are then noted and tested for the granular gas in Sec. IV. Since the underlying basis for these relations (time reversal symmetry) no longer holds for granular systems, the expected violation is demonstrated as a function of α for the same conditions. The stability of a special homogeneous solution to the mixture hydrodynamic equations is then studied, and some comments on the implications of the instability found are offered. Finally, the results are summarized and discussed in the last section.

II. BOLTZMANN KINETIC THEORY FOR THE MASS AND HEAT FLUXES

We consider a binary mixture of *inelastic*, smooth, hard spheres of masses m_1 and m_2, and diameters σ_1 and σ_2. The inelasticity of collisions among all pairs is characterized by three independent constant coefficients of normal restitution α_{11}, α_{22}, and $\alpha_{12}=\alpha_{21}$, where α_{ij} is the coefficient of restitution for collisions between particles of species i and j. It is assumed that the density of each species is sufficiently low that their velocity distribution functions are accurately described by the coupled set of *inelastic* Boltzmann kinetic equations. The precise form of these equations is given in Ref. 12 and will not be required here. These equations imply the exact macroscopic balance equations for the particle number density of each species $n_i(\mathbf{r},t)$, flow velocity $\mathbf{u}(\mathbf{r},t)$, and temperature $T(\mathbf{r},t)$ (Ref. 12),

$$D_t n_i + n_i \nabla\cdot\mathbf{u} + \frac{\nabla\cdot\mathbf{j}_i}{m_i} = 0, \quad i=1,2, \tag{1}$$

$$D_t\mathbf{u} + \rho^{-1}\nabla\cdot\mathsf{P} = 0, \tag{2}$$

$$D_t T - \frac{T}{n}\sum_i \frac{\nabla\cdot\mathbf{j}_i}{m_i} + \frac{2}{3n}(\nabla\cdot\mathbf{q} + \mathsf{P}:\nabla\mathbf{u}) = -\zeta T. \tag{3}$$

In the above equations, $D_t=\partial_t+\mathbf{u}\cdot\nabla$ is the material derivative, $\rho=m_1n_1+m_2n_2$ is the total mass density, $\mathbf{j}_i$ is the particle number flux for species i, $\mathbf{q}$ is the heat flux, P is the pressure tensor, and ζ is the cooling rate. For the two component mixture considered here there are six independent fields, n_1, n_2, T, $\mathbf{u}$. To obtain a closed set of hydrodynamic equations, expressions for $\mathbf{j}_i$, $\mathbf{q}$, P, and ζ must be given in terms of these fields. Such expressions are called "constitutive equations." It is convenient to give these constitutive equations in terms of a different set of experimentally more accessible fields, x_1, p, T, $\mathbf{u}$, where $x_1=n_1/(n_1+n_2)$ is the composition of species 1, and $p=(n_1+n_2)T$ is the hydrostatic pressure. This is simply a change of variables, so that Eqs. (1)–(3) become

$$D_t x_1 + \frac{\rho}{n^2 m_1 m_2}\nabla\cdot\mathbf{j}_1 = 0, \tag{4}$$

$$D_t p + p\nabla\cdot\mathbf{u} + \frac{2}{3}(\nabla\cdot\mathbf{q} + \mathsf{P}:\nabla\mathbf{u}) = -\zeta p, \tag{5}$$

$$D_t\mathbf{u} + \rho^{-1}\nabla\cdot\mathsf{P} = 0, \tag{6}$$

$$D_t T - \frac{T}{n}\sum_i \frac{\nabla\cdot\mathbf{j}_i}{m_i} + \frac{2}{3n}(\nabla\cdot\mathbf{q} + \mathsf{P}:\nabla\mathbf{u}) = -\zeta T. \tag{7}$$

The constitutive equations up to the Navier–Stokes order have been obtained from the Boltzmann equation in Ref. 12 with the results

$$\mathbf{j}_1 = -\left(\frac{m_1m_2n}{\rho}\right)D\nabla x_1 - \frac{\rho}{p}D_p\nabla p - \frac{\rho}{T}D'\nabla T,$$
$$\mathbf{j}_2 = -\mathbf{j}_1, \tag{8}$$

$$\mathbf{q} = -T^2D''\nabla x_1 - L\nabla p - \lambda\nabla T, \tag{9}$$

$$P_{k\ell} = p\delta_{k\ell} - \eta\left(\nabla_\ell u_k + \nabla_k u_\ell - \frac{2}{3}\delta_{k\ell}\nabla\cdot\mathbf{u}\right), \tag{10}$$

$$\zeta = \zeta_0 + \mathcal{O}(\nabla^2). \tag{11}$$

The transport coefficients $\{D,D_p,D',D'',L,\lambda,\eta\}$ verify a set of coupled linear integral equations which can be solved approximately by using the leading terms in a Sonine polynomial expansion. This solution provides explicit expressions for the transport coefficients in terms of the coefficients of restitution and the parameters of the mixture (masses, sizes, and composition). The above expressions for mass and heat fluxes can be defined in a variety of equivalent ways depending on the choice of driving forces used. For systems with elastic collisions, the specific set of gradients contributing to each flux is restricted by fluid symmetry, Onsager's relations (time reversal invariance), and the form of entropy production.[22] In this case, one usual representation leads to the mass and heat fluxes proportional to $(\nabla\mu_i)_T$ and ∇T, where μ_i (defined below) is the chemical potential per unit mass. However, for *inelastic* systems only fluid symmetry holds and so there is more flexibility in representing the fluxes and identifying the corresponding transport coefficients. In particular, a third contribution proportional to ∇p appears in both fluxes. Some care is required in comparing transport coefficients in different representations using different independent gradients for the driving forces.

The cooling rate to lowest order in the gradients is $\zeta=\zeta_0(x_1,p,T)$. There are no contributions to first order in the gradient for the low-density Boltzmann equation. The general form including second-order gradient contributions is displayed in the Appendix. These second-order terms have been calculated for a one-component gas[4] and found to be very small. Here, these second-order contributions to the cooling rate will be neglected.

Substitution of the Navier–Stokes constitutive equations, (8)–(10), into the exact balance equations, (4)–(7), gives the Navier–Stokes hydrodynamic equations for a binary mixture

$$D_t x_1 = \frac{\rho}{n^2 m_1 m_2} \nabla \cdot \left(\frac{m_1 m_2 n}{\rho} D \nabla x_1 + \frac{\rho}{p} D_p \nabla p + \frac{\rho}{T} D' \nabla T \right), \tag{12}$$

$$(D_t + \zeta) p + \frac{5}{3} p \nabla \cdot \mathbf{u} = \frac{2}{3} \nabla \cdot (T^2 D'' \nabla x_1 + L \nabla p + \lambda \nabla T) + \frac{2}{3} \eta \left(\nabla_\ell u_k + \nabla_k u_\ell - \frac{2}{3} \delta_{k\ell} \nabla \cdot \mathbf{u} \right) \nabla_\ell u_k, \tag{13}$$

$$(D_t + \zeta) T + \frac{2}{3} p \nabla \cdot \mathbf{u} = -\frac{T}{n} \frac{m_2 - m_1}{m_1 m_2} \nabla \cdot \left(\frac{m_1 m_2 n}{\rho} D \nabla x_1 + \frac{\rho}{p} D_p \nabla p + \frac{\rho}{T} D' \nabla T \right) + \frac{2}{3n} \nabla \cdot (T^2 D'' \nabla x_1 + L \nabla p + \lambda \nabla T), + \frac{2}{3n} \eta \left(\nabla_\ell u_k + \nabla_k u_\ell - \frac{2}{3} \delta_{k\ell} \nabla \cdot \mathbf{u} \right) \nabla_\ell u_k, \tag{14}$$

$$D_t u_\ell + \rho^{-1} \nabla_\ell p = \rho^{-1} \nabla_k \eta \left(\nabla_\ell u_k + \nabla_k u_\ell - \frac{2}{3} \delta_{k\ell} \nabla \cdot \mathbf{u} \right). \tag{15}$$

For the chosen set of fields $n = p/T$ and $\rho = p[(m_1 - m_2)x_1 + m_2]/T$. These equations are exact to second order in the spatial gradients for a low-density Boltzmann gas.

A. Mass flux

The mass flux contains three transport coefficients: the diffusion coefficient D, the pressure diffusion coefficient D_p, and the thermal diffusion coefficient D'. Explicit expressions for these were obtained in Ref. 12 using a first Sonine approximation. Dimensionless forms are defined by

$$D = \frac{\rho T}{m_1 m_2 \nu_0} D^*, \quad D_p = \frac{nT}{\rho \nu_0} D_p^*, \quad D' = \frac{nT}{\rho \nu_0} D'^*. \tag{16}$$

Here, $\nu_0 = \sqrt{\pi} n \sigma_{12}^2 v_0$, $\sigma_{12} = (\sigma_1 + \sigma_2)/2$, and $v_0 = \sqrt{2T(m_1 + m_2)/m_1 m_2}$ is a thermal velocity defined in terms of the temperature T of the mixture. The explicit forms are then

$$D^* = \left[\left(\frac{\partial}{\partial x_1} x_1 \gamma_1 \right)_{p,T} + \left(\frac{\partial \zeta^*}{\partial x_1} \right)_{p,T} \left(1 - \frac{\zeta^*}{2\nu^*} \right) D_p^* \right] \times \left(\nu^* - \frac{1}{2} \zeta^* \right)^{-1}, \tag{17}$$

$$D_p^* = x_1 \left[\gamma_1 - \frac{\mu(1+\delta)}{1+\mu\delta} \right] \left(\nu^* - \frac{3}{2} \zeta^* + \frac{\zeta^{*2}}{2\nu^*} \right)^{-1}, \tag{18}$$

$$D'^* = -\frac{\zeta^*}{2\nu^*} D_p^*. \tag{19}$$

In these equations,

$$\gamma_1 = \frac{T_1}{T} = \frac{\gamma}{1 + x_1(\gamma - 1)}, \quad \gamma_2 = \frac{T_2}{T} = \frac{1}{1 + x_1(\gamma - 1)}, \tag{20}$$

where $\mu = m_1/m_2$ is the mass ratio, $\mu_{ij} = m_i/(m_i + m_j)$, $\delta = x_1/x_2$, and $\gamma = T_1/T_2$. The detailed forms for the temperature ratio γ, dimensionless collision rate ν^*, and dimensionless cooling rate ζ^* are given in the Appendix. Since $\mathbf{j}_1 = -\mathbf{j}_2$ and $\nabla x_1 = -\nabla x_2$, it is expected that D^* should be symmetric with respect to interchange of particles 1 and 2 while D_p^* and D'^* should be antisymmetric. This can be easily verified by noting that $x_1 \gamma_1 + x_2 \gamma_2 = 1$.

In the case of elastic collisions $\alpha_{ij} = 1$, $\zeta^* = 0$, $\gamma = 1$, and Eqs. (17)–(19) become

$$D^* = \frac{3}{8} \frac{1 + \delta}{1 - \mu_{12}(1 - \delta)}, \quad D_p^* = x_1 \frac{(1 - \mu)}{1 + \mu\delta} D^*, \quad D'^* = 0. \tag{21}$$

These coincide with known results obtained for elastic collisions in the first Sonine approximation.[3] Recently, it has been shown that the estimate given by the first Sonine approximation for the diffusion coefficient D (in the very dilute concentration limit $x_1 \to 0$) compares quite well with Monte Carlo simulations,[14] except for the cases in which the gas particles are much heavier and/or much larger than impurities. For these extreme cases, the second Sonine approximation to D improves the accuracy of the kinetic theory results.[14]

B. Heat flux

The heat flux requires going up to the second Sonine approximation. The transport coefficients D'', L, and λ appearing in the heat flux (9) are given by[12]

$$D'' = -\frac{5}{2} \frac{n}{(m_1 + m_2)\nu_0} \times \left[\frac{x_1 \gamma_1^3}{\mu_{12}} d_1'' + \frac{x_2 \gamma_2^3}{\mu_{21}} d_2'' - \left(\frac{\gamma_1}{\mu_{12}} - \frac{\gamma_2}{\mu_{21}} \right) D^* \right], \tag{22}$$

$$L = -\frac{5}{2} \frac{T}{(m_1 + m_2)\nu_0} \times \left[\frac{x_1 \gamma_1^3}{\mu_{12}} \ell_1 + \frac{x_2 \gamma_2^3}{\mu_{21}} \ell_2 - \left(\frac{\gamma_1}{\mu_{12}} - \frac{\gamma_2}{\mu_{21}} \right) D_p^* \right], \tag{23}$$

$$\lambda = -\frac{5}{2} \frac{nT}{(m_1 + m_2)\nu_0} \times \left[\frac{x_1 \gamma_1^3}{\mu_{12}} \lambda_1 + \frac{x_2 \gamma_2^3}{\mu_{21}} \lambda_2 - \left(\frac{\gamma_1}{\mu_{12}} - \frac{\gamma_2}{\mu_{21}} \right) D'^* \right], \tag{24}$$

where the expressions for the (dimensionless) Sonine coefficients $\{d_i'', \ell_i, \lambda_i\}$ are displayed in the Appendix. In Eqs. (22)–(24) it is understood that the coefficients D^*, D_p^*, and D'^* are given by Eqs. (17)–(19), respectively (first Sonine

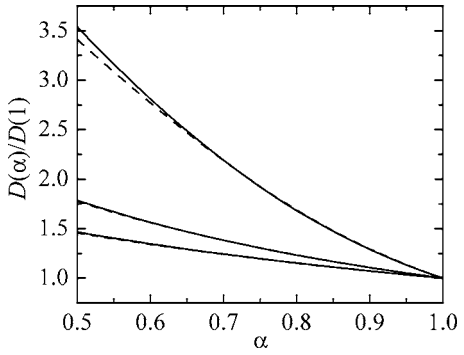

FIG. 1. Plot of the reduced mutual diffusion coefficient $D(\alpha)/D(1)$ as a function of the coefficient of restitution α for $x_1=0.2$, $\omega=1$, and $\mu=0.5$ (a), $\mu=1$ (b), and $\mu=4$ (c). The dashed lines correspond to the approximation $c_1=c_2=0$.

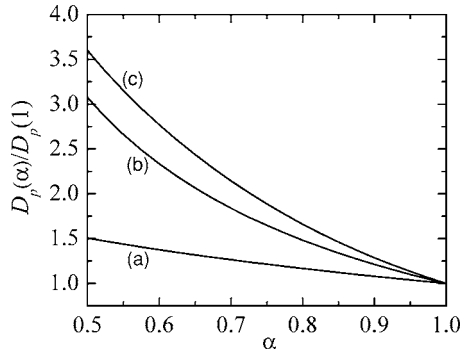

FIG. 2. Plot of the reduced pressure diffusion coefficient $D_p(\alpha)/D_p(1)$ as a function of the coefficient of restitution α for $x_1=0.2$, $\omega=1$, and $\mu=0.5$ (a), $\mu=2$ (b), and $\mu=4$ (c).

approximation). As expected, our results show that D'' is antisymmetric with respect to the change $1\leftrightarrow 2$ while L and λ are symmetric. Consequently, in the case of mechanically equivalent particles ($m_1=m_2\equiv m$, $\sigma_1=\sigma_2\equiv\sigma$, $\alpha_{ij}\equiv\alpha$), the coefficient D'' vanishes.

An equivalent representation is given in terms of the heat flow $\mathbf{J}_q$ defined as

$$\mathbf{J}_q \equiv \mathbf{q} - \frac{5}{2}T\sum_i \frac{\mathbf{j}_i}{m_i} = \mathbf{q} - \frac{5}{2}T\frac{m_2-m_1}{m_1m_2}\mathbf{j}_1, \tag{25}$$

where in the second equality use has been made of the requirement $\mathbf{j}_1=-\mathbf{j}_2$. The difference between $\mathbf{q}$ and $\mathbf{J}_q$ is a heat flow due to diffusion. In addition, for elastic collisions, $\mathbf{J}_q$ is the flux conjugate to the temperature gradient in the form of the entropy production where the contribution coming from the mass flux couples only to the gradient of the chemical potentials. The thermal conductivity in a mixture is generally measured in the absence of diffusion, i.e., when $\mathbf{j}_1=\mathbf{0}$. To identify this coefficient, we have to express $\mathbf{J}_q$ in terms of $\mathbf{j}_1$, ∇T, and ∇p. The corresponding coefficient of ∇T defines the thermal conductivity.[22] According to Eq. (8), the gradient of mole fraction ∇x_1 is

$$\nabla x_1 = -\frac{\rho}{m_1m_2nD}\mathbf{j}_1 - \frac{\rho^2}{m_1m_2p}\frac{D'}{D}\nabla T - \frac{\rho^2}{m_1m_2np}\frac{D_p}{D}\nabla p. \tag{26}$$

The expression of $\mathbf{J}_q$ is obtained by substituting Eq. (9) into Eq. (25) and eliminating ∇x_1 by using the identity (26). Thus, the heat flow is given by

$$\mathbf{J}_q = -\kappa\nabla T + \frac{\rho p}{m_1m_2n^2}\kappa_{\mathrm{T}}\mathbf{j}_1 - L_p\nabla p, \tag{27}$$

where

$$\kappa = \lambda - \frac{\rho^2T^2}{m_1m_2p}\frac{D''D'}{D}, \tag{28}$$

$$\kappa_{\mathrm{T}} = T\frac{D''}{D} - \frac{5}{2}\frac{n}{\rho}(m_2-m_1), \tag{29}$$

$$L_p = L - \frac{\rho^2T}{n^2m_1m_2}\frac{D''D_p}{D}. \tag{30}$$

As in the elastic case, the coefficient κ is the thermal conductivity while κ_{T} is called the thermal-diffusion factor or Dufour coefficient. There is a *new* contribution proportional to ∇p not present in the elastic case that defines the transport coefficient L_p.

For elastic collisions, $L_p=0$ (Ref. 23), and the expressions derived here for κ and κ_{T} coincide with those obtained for a gas-mixture of elastic hard spheres.[3] Furthermore, in the case of mechanically equivalent particles, the Dufour coefficient κ_{T} vanishes as expected and the heat flow (27) can be written as

$$\mathbf{J}_q = -\bar{\kappa}\nabla T - \bar{\mu}\nabla n, \tag{31}$$

where

$$\bar{\kappa} = \kappa + nL_p = \frac{25}{32}\left(\frac{mT}{\pi}\right)^{1/2}\sigma^{-2}\frac{1+c}{\nu_\kappa - 2\zeta^*}, \tag{32}$$

$$\bar{\mu} = TL_p = \frac{75}{32}\frac{T}{n}\left(\frac{mT}{\pi}\right)^{1/2}\sigma^{-2}\zeta^*\left(\frac{2}{3}\frac{1+c}{\nu_\kappa-2\zeta^*}+\frac{1}{3}\frac{c}{\zeta^*}\right)\times(2\nu_\kappa-3\zeta^*)^{-1}, \tag{33}$$

$$\nu_\kappa = \frac{1}{3}(1+\alpha)\left[1+\frac{33}{16}(1-\alpha)+\frac{19-3\alpha}{1024}c\right], \tag{34}$$

$$c = \frac{32(1-\alpha)(1-2\alpha^2)}{81-17\alpha+30\alpha^2(1-\alpha)}, \quad \zeta^* = \frac{5}{12}(1-\alpha^2)\left(1+\frac{3}{32}c\right). \tag{35}$$

Note that in writing Eq. (31) use has been made of the relation $\nabla p = n\nabla T + T\nabla n$. Equations (31)–(35) are the same as those obtained for the one-component granular gas.[4] This confirms the relevant known limiting cases for the granular mixture results described here.

III. TRANSPORT COEFFICIENTS

The transport coefficients depend on many parameters: $\{x_1, T, m_1/m_2, \sigma_1/\sigma_2, \alpha_{11}, \alpha_{22}, \alpha_{12}\}$. This complexity exists in the elastic limit as well, so the primary new feature is the

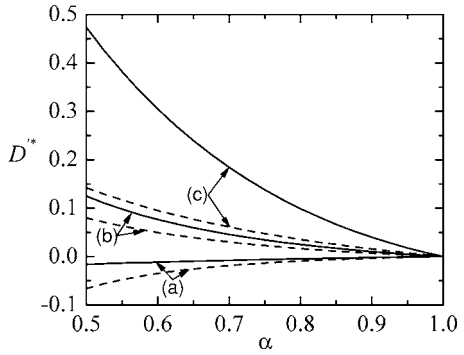

FIG. 3. Plot of the reduced thermal diffusion coefficient $D'^*(\alpha)$ as a function of the coefficient of restitution α for $x_1=0.2$, $\omega=1$, and $\mu=0.5$ (a), $\mu=2$ (b), and $\mu=4$ (c). The dashed lines correspond to $\gamma=1$.

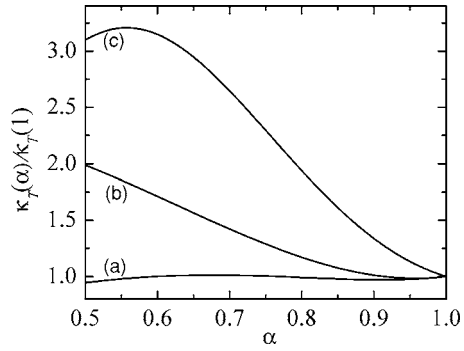

FIG. 5. Plot of the reduced Dufour coefficient $\kappa_T(\alpha)/\kappa_T(1)$ as a function of the coefficient of restitution α for $x_1=0.2$, $\omega=1$, and $\mu=0.5$ (a), $\mu=2$ (b), and $\mu=4$ (c).

dependence on the coefficients of restitution α_{ij} being different from unity. To illustrate the differences between granular and normal gases the transport coefficients are normalized to their values in the elastic limit. Then, the dependence on the overall temperature scales out. Also, only the simplest case of a common coefficient of restitution $(\alpha_{11}=\alpha_{22}=\alpha_{12}\equiv\alpha)$ and common size $\omega\equiv\sigma_1/\sigma_2=1$ is considered. This reduces the parameter set to three quantities: $\{m_1/m_2, x_1, \alpha\}$.

In Figs. 1–6, we plot the above transport coefficients as functions of the coefficient of restitution α for $x_1=0.2$, and several values of the mass ratio μ. It is understood that all coefficients have been reduced with respect to their elastic values, except in the cases of D' and L_p, since both coefficients vanish for elastic collisions. In these latter two cases, we have considered the reduced coefficients D'^* defined by Eq. (17) and $L_p^*=-[(5/2)T\nu_0/(m_1+m_2)]^{-1}L_p$. Figure 1 shows the mutual diffusion coefficient as a function of α for three mass ratios $\mu=0.5, 1$, and 4. There is a monotonic increase of the coefficient with decreasing α in all cases. Moreover, that effect increases as the mass of the dilute species increases. This is consistent with an observed singular behavior in the extreme case of tracer diffusion for a massive particle.[24] The velocity distributions in a granular gas are no longer Maxwellian,[8] and the difference is measured by the coefficients c_i that appear in the expressions for the transport coefficients.[12] The dashed curves in Fig. 1 correspond to $c_1=c_2\to 0$, the Maxwell limit. In this case it is seen that the distortion of the Maxwellian is not very important for this transport coefficient (see, however, discussion of Fig. 4 below). Figure 2 shows that the pressure diffusion coefficient has a very similar behavior. The thermal diffusion coefficient vanishes in the elastic limit and remains small and slightly negative when the dilute species has small mass ratio, as illustrated in Fig. 3. However, as the mass ratio becomes large it becomes large and positive for strong dissipation. The effect of different species temperatures is also shown on this graph. The dashed curves correspond to setting $\gamma=T_1/T_2\to 1$. This is seen to yield large errors, particularly in the case of large mass ratio (temperature differences are greater for mechanically different particles), indicating the real quantitative effect of two different species temperatures in granular gases.

The thermal conductivity is shown in Fig. 4, with the same monotonic increase with increasing dissipation. The dashed lines $(c_i=0)$ indicate a significant effect of the distortion of the reference distribution function from its Maxwellian form. Presumably, this is due to the fact that the thermal conductivity κ depends on a higher velocity moment than the mutual diffusion coefficient D and is more sensitive to the larger distortions at higher velocities. We also observe that there is little mass dependence when the dilute species is lighter. However, when the dilute species is more massive there is a significant decrease in the thermal conductivity, opposite to the case of diffusion. In contrast, the Dufour

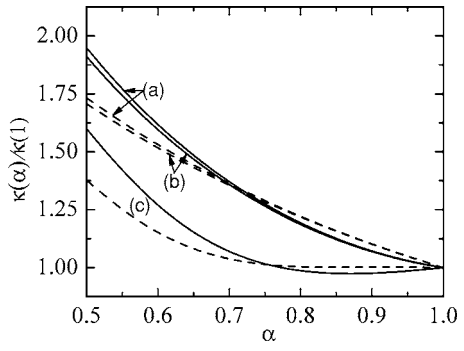

FIG. 4. Plot of the reduced thermal conductivity coefficient $\kappa(\alpha)/\kappa(1)$ as a function of the coefficient of restitution α for $x_1=0.2$, $\omega=1$, and $\mu=0.5$ (a), $\mu=1$ (b), and $\mu=4$ (c). The dashed lines correspond to the approximation $c_1=c_2=0$.

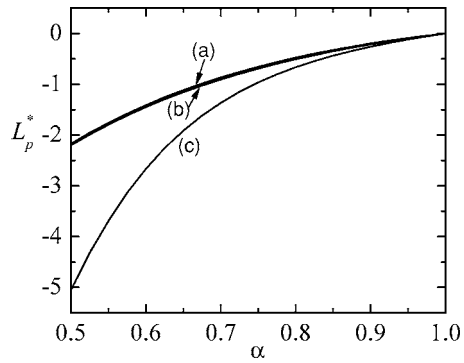

FIG. 6. Plot of the reduced coefficient $L_p^*(\alpha)$ as a function of the coefficient of restitution α for $x_1=0.2$, $\omega=1$, and $\mu=0.5$ (a), $\mu=1$ (b), and $\mu=4$ (c).

coefficient does have a dependence on the mass ratio more like diffusion (Fig. 5). Finally, the coefficient L_p^* is illustrated in Fig. 6. Again, there is weak dependence on the mass ratio until it becomes larger for the dilute species.

In summary, the mass and heat flux transport coefficients for a granular mixture differ significantly from those for a normal gas mixture even at moderate dissipation. In most cases (thermal conductivity is an exception) the differences increase with decreasing α, depend weakly on the mass ratio when the dilute species ($x_1/x_2<1$) is lighter than the excess species ($m_1/m_2\leq 1$), but increase significantly in the opposite case ($m_1/m_2>1$).

IV. ONSAGER'S RECIPROCAL RELATIONS

In the usual language of the linear irreversible thermodynamics for ordinary fluids,[22] the constitutive equations for the mass flux (8) and heat flow (27) are written

$$\mathbf{j}_i = -\sum_i L_{ij}\left(\frac{\nabla\mu_j}{T}\right)_T - L_{iq}\frac{\nabla T}{T^2} - C_p\nabla p, \tag{36}$$

$$\mathbf{J}_q = -L_{qq}\nabla T - \sum_i L_{qi}\left(\frac{\nabla\mu_i}{T}\right)_T - C_p'\nabla p, \tag{37}$$

where

$$\left(\frac{\nabla\mu_i}{T}\right)_T = \frac{1}{m_i}\nabla\ \ln(x_i p), \tag{38}$$

μ_i being the chemical potential per unit mass. Here, the coefficients L_{ij} are the so-called Onsager phenomenological coefficients. For *normal* fluids, Onsager showed[22] that time reversal invariance of the underlying microscopic equations of motion implies important restrictions on the above set of transport coefficients

$$L_{ij} = L_{ji}, \quad L_{iq} = L_{qi}, \quad C_p = C_p' = 0. \tag{39}$$

The first two symmetries are called reciprocal relations as they relate transport coefficients for different processes. The last two are statements that the pressure gradient does not appear in any of the fluxes even though it is admitted by symmetry. Even for a one-component fluid, Onsager's theorem is significant as it leads to Fourier's law for the heat flow rather than (31), i.e., $\bar{\mu}=0$. Since there is no time reversal symmetry for granular fluids, Eqs. (39) cannot be expected to apply. However, since explicit expressions for all transport coefficients are at hand, the quantitative extent of the violation can be explored.

To make a connection with the previous sections it is first necessary to transform Eqs. (36)–(38) to the variables x_1, p, T. Since $\nabla x_1=-\nabla x_2$, Eq. (38) implies

$$\frac{(\nabla\mu_1)_T-(\nabla\mu_2)_T}{T} = \frac{n\rho}{\rho_1\rho_2}\left[\nabla x_1 + \frac{n_1 n_2}{n\rho}(m_2-m_1)\nabla\ \ln p\right]. \tag{40}$$

The coefficients L_{ij} then can be easily obtained in terms of those of the previous sections. The result is

$$L_{11} = -L_{12} = -L_{21} = \frac{m_1 m_2 \rho_1\rho_2}{\rho^2}D, \quad L_{1q} = \rho T D', \tag{41}$$

$$L_{q1} = -L_{q2} = \frac{T^2\rho_1\rho_2}{n\rho}D'' - \frac{5}{2}\frac{T\rho_1\rho_2}{\rho^2}(m_2-m_1)D,$$

$$L_{qq} = \lambda - \frac{5}{2}\rho\frac{m_2-m_1}{m_1 m_2}D', \tag{42}$$

$$C_p \equiv \frac{\rho}{p}D_p - \frac{\rho_1\rho_2}{p\rho^2}(m_2-m_1)D, \tag{43}$$

$$C_p' \equiv L - \frac{5}{2}\frac{T}{p}\frac{m_2-m_1}{m_1 m_2}C_p - \frac{n_1 n_2}{np\rho}T^2(m_2-m_1)D''. \tag{44}$$

Onsager's relation $L_{12}=L_{21}$ is already evident since the diffusion coefficient D is symmetric under the change $1\leftrightarrow 2$, as discussed following Eq. (20).

Imposing Onsager's relation $L_{1q}=L_{q1}$ yields

$$D'' = \frac{5}{2}\frac{n}{T\rho}(m_2-m_1)D + \frac{n\rho^2}{T\rho_1\rho_2}D', \tag{45}$$

while the condition $C_p=C_p'=0$ leads to the following additional requirements:

$$D_p = \frac{\rho_1\rho_2}{\rho^3}(m_2-m_1)D, \tag{46}$$

$$\frac{5}{2}\frac{T}{p}(m_1-m_2)\left[\frac{n_1 n_2}{\rho^2}(m_2-m_1)D - \frac{\rho}{m_1 m_2}D_p\right] = pL - \frac{n_1 n_2}{n\rho}T^2(m_2-m_1)D''. \tag{47}$$

Since the relations (45)–(47) involve transport coefficients that have been determined in the first Sonine approximation, we restrict here our discussion to this level of approximation. In this case, $d_i''=\ell_i=\lambda_i=0$ so that Onsager's theorem, Eqs. (45)–(47), gives the conditions

$$P(\alpha_{ij}) \equiv [\gamma_1 - 1 + \mu(1-\gamma_2)]\frac{D^*}{\mu} + \frac{1}{5}\frac{(1+\delta)(1+\mu\delta)}{\mu\delta}\frac{\zeta^*}{\nu^*}D_p^* = 0, \tag{48}$$

$$Q(\alpha_{ij}) \equiv D_p^* - x_1\frac{(1-\mu)}{(1+\mu\delta)}D^* = 0, \tag{49}$$

$$R(\alpha_{ij}) \equiv \frac{1+\mu}{\mu}(\gamma_1 - \mu\gamma_2)Q(\alpha_{ij}) = 0. \tag{50}$$

In the elastic limit, the reduced coefficients D_p^* and D^* are given by Eq. (21) and these conditions are verified. Also, for mechanically equivalent particles with arbitrary α, $\gamma_i=1$ and $D_p^*=0$, so that $P(\alpha)=Q(\alpha)=R(\alpha)=0$. Nevertheless, beyond these limit cases, Onsager's relations do not apply (as expected). At this macroscopic level the origin of this failure is due to the cooling of the reference state as well as the occur-

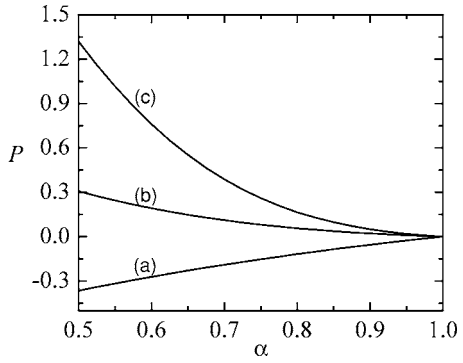

FIG. 7. Plot of $P(\alpha)$ as a function of α for $x_1=0.2$, $\omega=1$, and $\mu=0.5$ (a), $\mu=2$ (b), and $\mu=4$ (c).

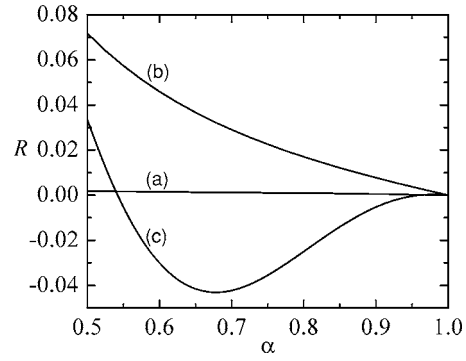

FIG. 9. Plot of $R(\alpha)$ as a function of α for $x_1=0.2$, $\omega=1$, and $\mu=0.5$ (a), $\mu=2$ (b), and $\mu=4$ (c).

rence of different kinetic temperatures for both species. Figures 7–9 show the dependence of the quantities P, Q, and R, respectively, on the (common) coefficient of restitution $\alpha_{ij}\equiv\alpha$ for mass ratios $\mu=0.5, 2$, and 4.

V. LINEARIZED HYDRODYNAMIC EQUATIONS AND STABILITY

In contrast to normal fluids, the Navier–Stokes hydrodynamic equations (12)–(15) have nontrivial solutions even for spatially homogeneous states,

$$\partial_t x_{1H}=0=\partial_t u_{H\ell}, \tag{51}$$

$$[\partial_t+\zeta(x_{1H},T_H,p_H)]T_H=0, \quad [\partial_t+\zeta(x_{1H},T_H,p_H)]p_H=0, \tag{52}$$

where the subscript H denotes the homogeneous state. Since the dependence of the cooling rate $\zeta(x_{1H},T_H,p_H)$ on x_{1H},T_H,p_H is known (see the Appendix), these first-order nonlinear equations can be solved for the time dependence of the homogeneous state. The result is the familiar Haff's cooling law for $T(t)$ at constant density.[2] As discussed above, each species temperature also has the same time dependence but each with a different value.[8] In this section, the hydrodynamics for small initial spatial perturbations of this homogeneous cooling state is discussed. For normal fluids such perturbations decay in time according to the hydrodynamic modes of diffusion (shear, thermal, mass) and damped sound propagation. The analysis is for fixed coefficients of restitution different from unity in the long wavelength limit. It will be seen here that the corresponding modes for a granular fluid are then quite different from those for a normal fluid. An alternative analysis with fixed long wavelength and coefficient of restitution approaching unity leads to usual normal fluid modes. Thus, the nature of hydrodynamic modes is nonuniform with respect to the inelasticity and the wavelength of the perturbation.

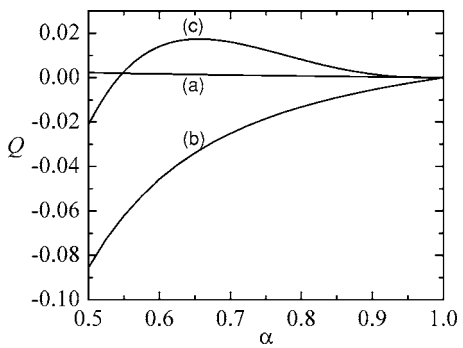

FIG. 8. Plot of $Q(\alpha)$ as a function of α for $x_1=0.2$, $\omega=1$, and $\mu=0.5$ (a), $\mu=2$ (b), and $\mu=4$ (c).

Let $\delta y_\alpha(\mathbf{r},t)=y_\alpha(\mathbf{r},t)-y_{H\alpha}(t)$ denote the deviation of $\{x_1,\mathbf{u},T,p\}$ from their values in the HCS. If the initial spatial perturbation is sufficiently small, then for some initial time interval these deviations will remain small and the hydrodynamic equations (12)–(15) can be linearized with respect to $\delta y_\alpha(\mathbf{r},t)$. This leads to partial differential equations with coefficients that are independent of space but which depend on time since the HCS is cooling. As in the one-component case,[4,25] this time dependence can be eliminated through a change in the time and space variables, and a scaling of the hydrodynamic fields. We introduce the following dimensionless space and time variables:

$$\tau=\int_0^t dt'\,\nu_H(t'), \quad \mathbf{r}'=\mathbf{r}/\ell_H, \tag{53}$$

where $v_{0H}=\sqrt{2T_H(m_1+m_2)/m_1m_2}$ is the thermal velocity introduced above, $\ell_H=1/\sqrt{\pi}n_H\sigma_{12}^2$ is an effective mean free path, and $\nu_H(t)=v_{0H}(t)/\ell_H$ is the effective collision frequency. The dimensionless time scale is therefore an average number of collisions up to the time t. A set of Fourier transformed dimensionless variables are then defined by

$$\delta y_{\mathbf{k}\alpha}(\tau)=\int d\mathbf{r}'e^{-i\mathbf{k}\cdot\mathbf{r}'}\delta y_\alpha(\mathbf{r}',\tau), \tag{54}$$

$$\rho_{\mathbf{k}}(\tau)=\frac{\delta x_{1\mathbf{k}}(\tau)}{x_{1H}}, \quad \mathbf{w}_{\mathbf{k}}(\tau)=\frac{\delta\mathbf{u}_{\mathbf{k}}(\tau)}{v_{0H}(\tau)}, \tag{55}$$

$$\theta_{\mathbf{k}}(\tau)=\frac{\delta T_{\mathbf{k}}(\tau)}{T_H(\tau)}, \quad \Pi_{\mathbf{k}}(\tau)=\frac{\delta p_{\mathbf{k}}(\tau)}{p_H(\tau)}. \tag{56}$$

In terms of these variables the linearized hydrodynamic equations for the set $\{\rho_{\mathbf{k}},\mathbf{w}_{\mathbf{k}},\theta_{\mathbf{k}},\Pi_{\mathbf{k}}\}$ separate into a

degenerate pair of equations for the two transverse velocity components $w_{\mathbf{k}\perp}$ (orthogonal to $\mathbf{k}$)

$$\left(\frac{\partial}{\partial\tau}-\frac{\zeta^*}{2}+\eta^* k^2\right)w_{\mathbf{k}\perp}=0, \tag{57}$$

and a coupled set of equations for $\rho_{\mathbf{k}}, \theta_{\mathbf{k}}, \Pi_{\mathbf{k}}$, and the longitudinal velocity component $w_{\mathbf{k}\|}$ (parallel to $\mathbf{k}$)

$$\frac{\partial \delta z_{\mathbf{k}\alpha}(\tau)}{\partial\tau}=\left(M^{(0)}_{\alpha\beta}+ikM^{(1)}_{\alpha\beta}+k^2M^{(2)}_{\alpha\beta}\right)\delta z_{\mathbf{k}\beta}(\tau), \tag{58}$$

where now $\delta z_{\mathbf{k}\alpha}(\tau)$ denotes the four variables $(\rho_{\mathbf{k}}, \theta_{\mathbf{k}}, \Pi_{\mathbf{k}}, w_{\mathbf{k}\|})$. The matrices in this equation are

$$M^{(0)}=\begin{pmatrix} 0 & 0 & 0 & 0 \\ -x_1\left(\frac{\partial\zeta^*}{\partial x_1}\right)_{T,p} & \frac{\zeta^*}{2}-\zeta^* & 0 \\ -x_1\left(\frac{\partial\zeta^*}{\partial x_1}\right)_{T,p} & \frac{\zeta^*}{2}-\zeta^* & 0 \\ 0 & 0 & 0 & \frac{\zeta^*}{2} \end{pmatrix}, \tag{59}$$

$$M^{(1)}=\begin{pmatrix} 0 & 0 & 0 & 0 \\ 0 & 0 & 0 & -\frac{2}{3} \\ 0 & 0 & 0 & -\frac{5}{3} \\ 0 & 0 & -\frac{1}{2}\frac{\mu_{12}}{x_1\mu+x_2} & 0 \end{pmatrix}, \tag{60}$$

$$M^{(2)}=\begin{pmatrix} -\frac{1}{2}\frac{\mu x_1+x_2}{1+\mu}D^* & -\frac{1}{2x_1}\frac{\mu x_1+x_2}{1+\mu}D'^* & -\frac{1}{2x_1}\frac{\mu x_1+x_2}{1+\mu}D_p^* & 0 \\ -x_1\left(\frac{2}{3}D''^*-\frac{1-\mu}{2(1+\mu)}D^*\right) & \frac{1-\mu}{2(1+\mu)}D'^*-\frac{2}{3}\lambda^* & -\frac{2}{3}L^*+\frac{1-\mu}{2(1+\mu)}D_p^* & 0 \\ -\frac{2}{3}x_1D''^* & -\frac{2}{3}\lambda^* & -\frac{2}{3}L^* & 0 \\ 0 & 0 & 0 & -\frac{4}{3}\eta^* \end{pmatrix}. \tag{61}$$

In these equations, $x_i=n_{iH}/n_H$, $\zeta^*=\zeta_H/\nu_H$, and the reduced transport coefficients D^*, D_p^*, and D'^* are given by Eqs. (17)–(19), respectively. Moreover, the reduced Navier–Stokes transport coefficients are

$$\eta^*=\frac{\nu_H\eta}{\rho_H v_{0H}^2}, \tag{62}$$

$$D''^*=\frac{\nu_H T_H D''}{n_H v_{0H}^2}, \quad L^*=\frac{\nu_H L}{v_{0H}^2}, \quad \lambda^*=\frac{\nu_H\lambda}{n_H v_{0H}^2}, \tag{63}$$

where $\rho_H=m_1n_{1H}+m_2n_{2H}$.

It is instructive to consider first the solutions to these equations in the extreme long wavelength limit, $k=0$. In this case, the eigenvalues or hydrodynamic modes are given by

$$s_\perp=\frac{1}{2}\zeta^*, \quad s_n=\left(0,0,-\frac{1}{2}\zeta^*,\frac{1}{2}\zeta^*\right), \tag{64}$$

where s_n refers to the longitudinal modes. Two of the eigenvalues are positive, corresponding to growth of the initial perturbation in time. Thus, some of the solutions are unstable. The two zero eigenvalues represent marginal stability solutions, while the negative eigenvalue gives stable solutions. For general initial perturbations all modes are excited. These modes correspond to evolution of the fluid due to uniform perturbations of the HCS, i.e., a global change in the HCS parameters. The unstable modes are seen to arise from the initial perturbations $w_{\mathbf{k}\perp}(0)$ or $w_{\mathbf{k}\|}(0)$. The marginal modes correspond to changes in the composition at fixed pressure, density, and velocity, and to changes in $\Pi_{\mathbf{k}}-\theta_{\mathbf{k}}$ at constant composition and velocity. The decaying mode corresponds to changes in the temperature or pressure for $\Pi_{\mathbf{k}}=\theta_{\mathbf{k}}$. The unstable modes may appear trivial since they are due entirely to the normalization of the fluid velocity by the time-dependent thermal velocity. However, this normalization is required by the scaling of the entire set of equations to obtain time-independent coefficients.

At finite wave vectors, these instabilities give rise to real growth of spatial perturbations. The linear growth of the transverse modes is simply given by

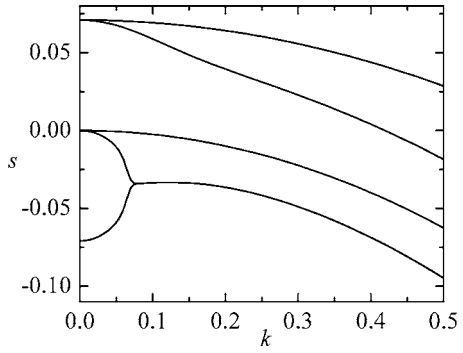

FIG. 10. Dispersion relations for $\alpha=0.9$, $x_1=0.2$, $\omega=1$, and $\mu=4$.

$$w_{\mathbf{k}\perp}(\tau)=w_{\mathbf{k}\perp}(0)\exp\left(\frac{1}{2}\zeta^*-\eta^* k^2\right)\tau. \tag{65}$$

The instability for the two shear modes is removed at sufficiently large $k>k_\perp^c$, where

$$k_\perp^c=\left(\frac{\zeta^*}{2\eta^*}\right)^{1/2}. \tag{66}$$

The wave vector dependence of the remaining four modes is more complex. This is illustrated in Fig. 10 showing the real parts of the modes $s(k)$ for $\alpha_{ij}=0.9$, $\sigma_1/\sigma_2=1$, $x_1=0.2$, and $m_1/m_2=4$. The $k=0$ values are those of (64), corresponding to six hydrodynamic modes with two different degeneracies. The shear mode degeneracy remains at finite k but the other is removed at any finite k. At sufficiently large k a pair of real modes becomes equal and becomes a complex conjugate pair at all larger wave vectors, like a sound mode. The smaller of the unstable modes is that associated with the longitudinal velocity, which couples to the scalar hydrodynamic fields. It becomes negative at a wave vector smaller than that of Eq. (66) and gives the threshold for development of spatial instabilities.

The results obtained here for the mixture show no new surprises relative to the earlier work for a one-component gas,[4,25] with only the addition of the stable mass diffusion mode. Of course, the quantitative features can be quite different since there are additional degrees of freedom with the parameter set $\{x_1, T, m_1/m_2, \sigma_1/\sigma_2, \alpha_{ij}\}$. Also, the manner in which these linear instabilities are enhanced by the nonlinearities may be different from that for the one-component case.

VI. SUMMARY AND DISCUSSION

The Navier–Stokes order hydrodynamic equations have been discussed for a low-density granular binary mixture. The form of the momentum flux is the same as for a one-component gas, with only the value of the viscosity changed (see the Appendix). Since the dependence of the viscosity on the parameters of the mixture has been widely explored in a previous paper,[13] attention has been focused here on the mass and heat fluxes and their associated transport coefficients. There is no phenomenology involved as the equations and the transport coefficients have been derived systematically from the inelastic Boltzmann equation by the Chapman-Enskog procedure. Consequently, there is no *a priori* limitation on the degree of inelasticity, size and mass ratios, or composition. For practical purposes, the integral equations determining the transport coefficients have been solved by truncated expansions in Sonine polynomials. This is expected to fail at extreme values of size or mass ratio,[13,14] but the results are quite accurate otherwise.

The hydrodynamic equations are the same as for a normal gas, except for a sink in the energy equation due to granular cooling, and additional transport coefficients in the mass and heat flux constitutive equations. The latter arise because the usual restrictions of irreversible thermodynamics no longer apply. These restrictions include Onsager reciprocal relations among various transport coefficients, and the extent to which these are violated has been demonstrated in Sec. IV. It has been verified that the results described here reduce to those for a normal mixture in the elastic limit,[3] and to those for a one-component granular gas[4] when the species are mechanically identical.

As is the case for a normal gas, the hydrodynamic fields include only the global temperature even though two species temperatures can be defined. For a normal gas the species temperatures rapidly approach the global temperature due to equipartition. For the granular gas the species temperatures approach different values, but with the same time dependence as the global temperature. The transport coefficients have an additional dependence on the composition due to this time-independent ratio of species temperatures. This has been illustrated in Fig. 3 for the thermal diffusion coefficient, where the effect is seen to be large for large mass ratio (implying very different species temperatures). Generally, it was seen that the deviation due to inelasticity is enhanced for greater mechanical differences between the species.

The linear equations for small perturbations of the special homogeneous cooling solution to the hydrodynamic equations were obtained and discussed. In order to characterize the solutions in terms of modes, it is necessary to introduce dimensionless fields so that the time dependence of the reference HCS is eliminated. The resulting equations exhibit a long wavelength instability for three of the modes. This is quite similar to the case of a one-component granular gas,[4,25] and in fact the same modes are unstable here. The additional diffusion mode for two species behaves as for a normal fluid. The consequences of this instability for a binary mixture were not studied here. This entails an analysis of the dominant nonlinearities, which has not been performed as yet. Since there are additional degrees of freedom it would be interesting to see if the density clustering that occurs for a one-component system is more complex here (e.g., species segregation).

Hydrodynamics derived from hard-sphere models has found widespread use in the description of numerous industrial processes involving solid particles. Of particular relevance are high-speed, gas-solid flows as found in pneumatic conveyors (of ores, chemicals, grains, etc.) and fluidized beds (for fluid catalytic cracking, power generation, granulation of pharmaceutical powders, synthesis of fine chemicals such as titania, etc.). Such descriptions are now standard features of commercial, multiphase computational fluid dynam-

ics codes like Fluent™ and open-source, research codes like MFIX (www.mfix.org). Such codes rely upon accurate transport properties and a first-order objective is to assure this accuracy from a careful theoretical treatment. The price of this approach, in contrast to more phenomenological approaches, is an increasing complexity of the expressions as the systems become more complex. It would be useful if some universal features could be identified for mathematically simpler and more transparent modeling. This is a difficult objective even for normal molecular mixtures. The analysis here has focused on exploring some of the central differences from such mixtures that occur for granular gases. The longer term objective, underway, is to extend the present results to moderately dense, polydisperse mixtures based on the Enskog kinetic equation. The precise expressions for transport coefficients will be even more complex, due to the expanded parameter space. Of course, this complexity is not a problem for implementation in a code. Ultimately, a public website is planned for extraction of transport properties under the users' chosen state conditions.

ACKNOWLEDGMENTS

The authors are indebted to Christine Hrenya for helpful comments. Partial support of the Ministerio de Ciencia y Tecnología (Spain) through Grant No. FIS2004-01399 (partially financed by FEDER funds) in the case of V.G., and Grant No. ESP2003-02859 (partially financed by FEDER funds) in the case of J.M.M., is acknowledged. V.G. also acknowledges support from the European Community's Human Potential Programme HPRN-CT-2002-00307 (DYGLAGEMEM).

APPENDIX: SOME EXPLICIT EXPRESSIONS

Navier–Stokes hydrodynamics retains terms up through second order in the gradients. As a scalar, the cooling rate has the most general form at this order given by

$$\zeta = \zeta_0 + \zeta_u \nabla\cdot\mathbf{u} + \zeta_x\nabla^2 x_1 + \zeta_T\nabla^2 T + \zeta_p\nabla^2 p + \zeta_{TT}(\nabla T)^2 + \zeta_{xx}(\nabla x_1)^2 + \zeta_{pp}(\nabla p)^2 + \zeta_{Tx}(\nabla T)\cdot(\nabla x_1) + \zeta_{Tp}(\nabla T)\cdot(\nabla p) + \zeta_{px}(\nabla p)\cdot(\nabla x_1) + \zeta_{uu}(\nabla_i u_j)(\nabla_i u_j). \tag{A1}$$

For a low-density gas the first-order gradient term vanishes,[4] $\zeta_u=0$. However, for higher densities ζ_u is different from zero.[26] The second-order terms have been left implicit in Eqs. (13) and (14) for the temperature and the pressure. As noted in the text, these second-order terms have been calculated for a one-component fluid[4] and found to be very small relative to corresponding terms from the fluxes. Consequently, they have been neglected in the linearized hydrodynamic equations (58).

1. Mass flux parameters

The transport coefficients are expressed in terms of a number of dimensionless parameters. For completeness, they are listed here. In general they depend on the reference distribution functions in the Chapman–Enskog expansion, which are not Maxwellians.[8] The deviation of the reference distributions from their Maxwellian forms is measured by the cumulants c_i.[8] As shown in Sec. III, while the influence of these coefficients on the transport coefficients is not quite important in the case of the coefficients associated with the mass flux (see Fig. 1, for example), it is not the same in the case of the heat flux (see Fig. 4, for example), where the influence of c_i is not negligible for strong dissipation. However, in order to offer a simplified theory the parameters given in this appendix have neglected the corrections due to the cumulants c_i. The full expressions for the transport coefficients can be found in Ref. 12.

The temperature ratio $\gamma=T_1/T_2$ is determined from the condition

$$\zeta_1^* = \zeta_2^* = \zeta^*, \tag{A2}$$

where the dimensionless cooling rate, $\zeta_i^*=\zeta_i/\nu_0$ [ν_0 is the average frequency defined below (16)], is

$$\zeta_1^* = \frac{2}{3}\sqrt{2\pi}\left(\frac{\sigma_1}{\sigma_{12}}\right)^2 x_1\theta_1^{-1/2}(1-\alpha_{11}^2) + \frac{4}{3}\sqrt{\pi}x_2\mu_{21}\left(\frac{1+\theta}{\theta}\right)^{1/2}(1+\alpha_{12})\theta_2^{-1/2} \times[2-\mu_{21}(1+\alpha_{12})(1+\theta)]. \tag{A3}$$

The expression for ζ_2^* can be easily obtained by interchanging $1\leftrightarrow 2$. Here, $\theta_1=1/(\mu_{21}\gamma_1)$, $\theta_2=1/(\mu_{12}\gamma_2)$, $\mu_{ij}=m_i/(m_i+m_j)$, $\delta=x_1/x_2$, and $\theta=\theta_1/\theta_2=\mu/\gamma$. The temperature ratios γ_i are related to the temperature ratio γ through Eqs. (20). In the quasielastic limit ($\alpha_{ij}\ll 1$), the temperature ratio γ has the simple form

$$\gamma \to 1 + \frac{1}{2\mu_{12}\mu_{21}}\left\{(\mu_{12}x_1-\mu_{21}x_2)(1-\alpha_{12}) + \frac{1}{\sqrt{2}}\left[\left(\frac{\sigma_2}{\sigma_{12}}\right)^2 x_2\sqrt{\mu_{12}}(1-\alpha_{22}) - \left(\frac{\sigma_1}{\sigma_{12}}\right)^2 x_1\sqrt{\mu_{21}}(1-\alpha_{11})\right]\right\}. \tag{A4}$$

In this limit, the temperature ratio is a linear function of the hydrodynamic field x_1. The dimensionless frequency ν^* appearing in the expressions of the transport coefficients associated with the mass flux is

$$\nu^* = \frac{4}{3}\mu_{21}\frac{1+\mu\delta}{1+\delta}\left(\frac{1+\theta}{\theta}\right)^{1/2}\theta_2^{-1/2}(1+\alpha_{12}). \tag{A5}$$

The cooling rate ζ^* and frequency ν^* are also functions of the hydrodynamic field x_1. However, all the parameters above are independent of the temperature and density.

2. Heat and momentum flux parameters

As in the last section effects due to the distortion of the reference Maxwellian are neglected. In the case of the heat flux **q**, Eq. (9), the transport coefficients D'', L, and λ are given by Eqs. (22)–(24), respectively. By using matrix notation, the (dimensionless) Sonine coefficients d_i'', ℓ_i, and λ_i verify the coupled set of six equations[12]

$$\Lambda_{\sigma\sigma'} X_{\sigma'} = Y_\sigma, \tag{A6}$$

where $X_{\sigma'}$ is the column matrix

$$\mathbf{X} = \begin{pmatrix} d_1'' \\ d_2'' \\ \ell_1 \\ \ell_2 \\ \lambda_1 \\ \lambda_2 \end{pmatrix}, \tag{A7}$$

and $\Lambda_{\sigma\sigma'}$ is the matrix

$$\Lambda = \begin{pmatrix} \nu_{11} - \frac{3}{2}\zeta^* & \nu_{12} & -\left(\frac{\partial \zeta^*}{\partial x_1}\right)_{p,T} & 0 & -\left(\frac{\partial \zeta^*}{\partial x_1}\right)_{p,T} & 0 \\ \nu_{21} & \nu_{22} - \frac{3}{2}\zeta^* & 0 & -\left(\frac{\partial \zeta^*}{\partial x_1}\right)_{p,T} & 0 & -\left(\frac{\partial \zeta^*}{\partial x_1}\right)_{p,T} \\ 0 & 0 & \nu_{11} - \frac{5}{2}\zeta^* & \nu_{12} & -\zeta^* & 0 \\ 0 & 0 & \nu_{21} & \nu_{22} - \frac{5}{2}\zeta^* & 0 & -\zeta^* \\ 0 & 0 & \zeta^*/2 & 0 & \nu_{11} - \zeta^* & \nu_{12} \\ 0 & 0 & 0 & \zeta^*/2 & \nu_{21} & \nu_{22} - \zeta^* \end{pmatrix}. \tag{A8}$$

The column matrix Y_σ has the elements

$$Y_1 = D^*\left(\tau_{12} - \frac{\zeta^*}{x_1\gamma_1^2}\right) - \frac{1}{\gamma_1^2}\left(\frac{\partial \gamma_1}{\partial x_1}\right)_{p,T},$$

$$Y_2 = -D^*\left(\tau_{21} - \frac{\zeta^*}{x_2\gamma_2^2}\right) - \frac{1}{\gamma_2^2}\left(\frac{\partial \gamma_2}{\partial x_1}\right)_{p,T}, \tag{A9}$$

$$Y_3 = D_p^*\left(\tau_{12} - \frac{\zeta^*}{x_1\gamma_1^2}\right), \quad Y_4 = -D_p^*\left(\tau_{21} - \frac{\zeta^*}{x_2\gamma_2^2}\right), \tag{A10}$$

$$Y_5 = -\frac{1}{\gamma_1} + D'^*\left(\tau_{12} - \frac{\zeta^*}{x_1\gamma_1^2}\right),$$

$$Y_6 = -\frac{1}{\gamma_2} - D'^*\left(\tau_{21} - \frac{\zeta^*}{x_2\gamma_2^2}\right). \tag{A11}$$

The dimensionless collision integrals τ_{12}, ν_{11}, and ν_{12} are given, respectively, by

$$\tau_{12} = \frac{4}{3}\sqrt{\frac{\mu_{21}}{2}}\left(\frac{\sigma_1}{\sigma_{12}}\right)^2 \gamma_1^{-3/2}(1-\alpha_{11}^2) + \frac{4}{15}\mu_{21}^{-1}\gamma_1^{-4}(1+\alpha_{12}) \times (\theta_1+\theta_2)^{-1/2}(\theta_1\theta_2)^{-3/2}\left(\frac{x_2}{x_1}A - \gamma B\right), \tag{A12}$$

$$\nu_{11} = \frac{16}{15}x_1\left(\frac{\sigma_1}{\sigma_{12}}\right)^2 (2\theta_1)^{-1/2}(1+\alpha_{11})\left[1 + \frac{33}{16}(1-\alpha_{11})\right] + \frac{2}{15}x_2\mu_{21}(1+\alpha_{12})\left(\frac{\theta_1}{\theta_2(\theta_1+\theta_2)}\right)^{3/2} \times \left(E - 5\frac{\theta_1+\theta_2}{\theta_1}A\right), \tag{A13}$$

$$\nu_{12} = -\frac{2}{15}x_2\frac{\mu_{21}^2}{\mu_{12}}(1+\alpha_{12})\left(\frac{\theta_1}{\theta_2(\theta_1+\theta_2)}\right)^{3/2} \times \left(F + 5\frac{\theta_1+\theta_2}{\theta_2}B\right). \tag{A14}$$

In the above equations we have introduced the quantities[27]

$$A = 5(2\beta_{12}+\theta_2) + \mu_{21}(\theta_1+\theta_2)[5(1-\alpha_{12}) - 2(7\alpha_{12}-11)\beta_{12}\theta_1^{-1}] + 18\beta_{12}^2\theta_1^{-1} + 2\mu_{21}^2 \times (2\alpha_{12}^2 - 3\alpha_{12} + 4)\theta_1^{-1}(\theta_1+\theta_2)^2 - 5\theta_2\theta_1^{-1}(\theta_1+\theta_2), \tag{A15}$$

$$B = 5(2\beta_{12}-\theta_1) + \mu_{21}(\theta_1+\theta_2)[5(1-\alpha_{12}) + 2(7\alpha_{12}-11)\beta_{12}\theta_2^{-1}] - 18\beta_{12}^2\theta_2^{-1} - 2\mu_{21}^2 \times (2\alpha_{12}^2 - 3\alpha_{12} + 4)\theta_2^{-1}(\theta_1+\theta_2)^2 + 5(\theta_1+\theta_2), \tag{A16}$$

$$E = 2\mu_{21}^2\theta_1^{-2}(\theta_1+\theta_2)^2(2\alpha_{12}^2-3\alpha_{12}+4)(5\theta_1+8\theta_2) - \mu_{21}(\theta_1+\theta_2)[2\beta_{12}\theta_1^{-2}(5\theta_1+8\theta_2)(7\alpha_{12}-11) + 2\theta_2\theta_1^{-1}(29\alpha_{12}-37)-25(1-\alpha_{12})] + 18\beta_{12}^2\theta_1^{-2} \times(5\theta_1+8\theta_2) + 2\beta_{12}\theta_1^{-1}(25\theta_1+66\theta_2) + 5\theta_2\theta_1^{-1} \times(11\theta_1+6\theta_2) - 5(\theta_1+\theta_2)\theta_1^{-2}\theta_2(5\theta_1+6\theta_2), \quad \text{(A17)}$$

$$F = 2\mu_{21}^2\theta_2^{-2}(\theta_1+\theta_2)^2(2\alpha_{12}^2-3\alpha_{12}+4)(8\theta_1+5\theta_2) - \mu_{21}(\theta_1+\theta_2)[2\beta_{12}\theta_2^{-2}(8\theta_1+5\theta_2)(7\alpha_{12}-11) - 2\theta_1\theta_2^{-1}(29\alpha_{12}-37)+25(1-\alpha_{12})] + 18\beta_{12}^2\theta_2^{-2} \times(8\theta_1+5\theta_2) - 2\beta_{12}\theta_2^{-1}(66\theta_1+25\theta_2) + 5\theta_1\theta_2^{-1} \times(6\theta_1+11\theta_2) - 5(\theta_1+\theta_2)\theta_2^{-1}(6\theta_1+5\theta_2). \quad \text{(A18)}$$

Here, $\beta_{12}=\mu_{12}\theta_2-\mu_{21}\theta_1$. The corresponding expressions for τ_{21}, ν_{22}, and ν_{21} can be inferred from Eqs. (A12)–(A18) by interchanging $1\leftrightarrow 2$. For elastic collisions, the expressions (A12)–(A18) reduce to those obtained for hard-sphere mixtures.[28]

The solution to Eq. (A6) is

$$X_\sigma = (\Lambda^{-1})_{\sigma\sigma'}Y_{\sigma'}. \quad \text{(A19)}$$

This relation provides an explicit expression for the coefficients d_i'', ℓ_i, and λ_i in terms of the coefficients of restitution and the parameters of the mixture. Their explicit forms are

$$d_1'' = \frac{1}{\Delta}\Bigg\{2[2\nu_{12}Y_2 - Y_1(2\nu_{22}-3\zeta^*)][\nu_{12}\nu_{21}-\nu_{11}\nu_{22} + 2(\nu_{11}+\nu_{22})\zeta^* - 4\zeta^{*2}] + 2\left(\frac{\partial\zeta^*}{\partial x_1}\right)_{p,T}(Y_3+Y_5) \times[2\nu_{12}\nu_{21}+2\nu_{22}^2-\zeta^*(7\nu_{22}-6\zeta^*)] - 2\nu_{12}\left(\frac{\partial\zeta^*}{\partial x_1}\right)_{p,T}(Y_4+Y_6)(2\nu_{11}+2\nu_{22}-7\zeta^*)\Bigg\}, \quad \text{(A20)}$$

$$\ell_1 = \frac{1}{\Delta}\{-2Y_3[2(\nu_{12}\nu_{21}-\nu_{11}\nu_{22})\nu_{22}+\zeta^*(7\nu_{11}\nu_{22} - 5\nu_{12}\nu_{21}+2\nu_{22}^2-6\nu_{11}\zeta^*-7\nu_{22}\zeta^*+6\zeta^{*2})] + 2Y_4\nu_{12}[2\nu_{12}\nu_{21}-2\nu_{11}\nu_{22}+2\zeta^*(\nu_{11}+\nu_{22})-\zeta^{*2}] + 2Y_5\zeta^*[2\nu_{12}\nu_{21}+\nu_{22}(2\nu_{22}-7\zeta^*)+6\zeta^{*2}] - 2\nu_{12}\zeta^*Y_6[2(\nu_{11}+\nu_{22})-7\zeta^*]\}, \quad \text{(A21)}$$

$$\lambda_1 = \frac{1}{\Delta}\{-Y_3\zeta^*[2\nu_{12}\nu_{21}+\nu_{22}(2\nu_{22}-7\zeta^*)+6\zeta^{*2}] + \nu_{12}\zeta^*Y_4[2(\nu_{11}+\nu_{22})-7\zeta^*] - Y_5[4\nu_{12}\nu_{21}(\nu_{22}-\zeta^*) + 2\nu_{22}^2(5\zeta^*-2\nu_{11}) + 2\nu_{11}(7\nu_{22}\zeta^*-6\zeta^{*2})+5\zeta^{*2} \times(6\zeta^*-7\nu_{22})] + \nu_{12}Y_6[4\nu_{12}\nu_{21}+2\nu_{11}(5\zeta^*-2\nu_{22}) + \zeta^*(10\nu_{22}-23\zeta^*)]\}, \quad \text{(A22)}$$

where

$$\Delta = [4(\nu_{12}\nu_{21}-\nu_{11}\nu_{22})+6\zeta^*(\nu_{11}+\nu_{22})-9\zeta^{*2}] \times[\nu_{12}\nu_{21}-\nu_{11}\nu_{22}+2\zeta^*(\nu_{11}+\nu_{22})-4\zeta^{*2}]. \quad \text{(A23)}$$

The expressions for d_2'', ℓ_2, and λ_2 can be obtained from Eqs. (A20)–(A22) by setting $1\leftrightarrow 2$. From the above expressions one can easily get the transport coefficients D'', L, and λ from Eqs. (A22)–(A24), respectively. They are functions of x_1 but independent of temperature and pressure.

The pressure tensor $P_{k,\ell}$ is given by

$$P_{k\ell} = p\delta_{k\ell} - \eta\left(\nabla_\ell u_k + \nabla_k u_\ell - \frac{2}{3}\delta_{k\ell}\nabla\cdot\mathbf{u}\right), \quad \text{(A24)}$$

where η is the shear viscosity coefficient. Its expression can be written as[12]

$$\eta = \frac{nT}{\nu_0}(x_1\gamma_1^2\eta_1 + x_2\gamma_2^2\eta_2), \quad \text{(A25)}$$

with

$$\eta_1 = \frac{2\gamma_2(2\lambda_{22}-\zeta^*)-4\gamma_1\lambda_{12}}{\gamma_1\gamma_2[\zeta^{*2}-2\zeta^*(\lambda_{11}+\lambda_{22})+4(\lambda_{11}\lambda_{22}-\lambda_{12}\lambda_{21})]}, \quad \text{(A26)}$$

$$\eta_2 = \frac{2\gamma_1(2\lambda_{11}-\zeta^*)-4\gamma_2\lambda_{21}}{\gamma_1\gamma_2[\zeta^{*2}-2\zeta^*(\lambda_{11}+\lambda_{22})+4(\lambda_{11}\lambda_{22}-\lambda_{12}\lambda_{21})]}. \quad \text{(A27)}$$

The dimensionless quantities λ_{ij} are given by[12,13]

$$\lambda_{11} = \frac{16}{5\sqrt{2}}x_1\left(\frac{\sigma_1}{\sigma_{12}}\right)^2\theta_1^{1/2}\left[1-\frac{1}{4}(1-\alpha_{11})^2\right] + \frac{8}{15}x_2\mu_{21}(1+\alpha_{12})\theta_1^{3/2}\theta_2^{-1/2}\Bigg[6\theta_1^{-2}(\mu_{12}\theta_2-\mu_{21}\theta_1) \times(\theta_1+\theta_2)^{-1/2} + \frac{3}{2}\mu_{21}\theta_1^{-2}(\theta_1+\theta_2)^{1/2}(3-\alpha_{12}) + 5\theta_1^{-1} \times(\theta_1+\theta_2)^{-1/2}\Bigg], \quad \text{(A28)}$$

$$\lambda_{12} = \frac{8}{15}x_2\frac{\mu_{21}^2}{\mu_{12}}(1+\alpha_{12})\theta_1^{3/2}\theta_2^{-1/2}\Bigg[6\theta_2^{-2}(\mu_{12}\theta_2-\mu_{21}\theta_1) \times(\theta_1+\theta_2)^{-1/2} + \frac{3}{2}\mu_{21}\theta_2^{-2}(\theta_1+\theta_2)^{1/2}(3-\alpha_{12}) - 5\theta_2^{-1}(\theta_1+\theta_2)^{-1/2}\Bigg]. \quad \text{(A29)}$$

The corresponding expressions for λ_{22} and λ_{21} can be inferred from Eqs. (A26) and (A27) by interchanging $1\leftrightarrow 2$.

The program for calculating the cooling rates, the temperature ratio, and the transport coefficients of the binary mixture can be obtained on request from the authors.

[1] A. Goldshtein and M. Shapiro, "Mechanics of collisional motion of granular materials. Part 1. General hydrodynamic equations," J. Fluid Mech. **282**, 41 (1995); J. J. Brey, J. W. Dufty, and A. Santos, "Dissipative dynamics for hard spheres," J. Stat. Phys. **87**, 1051 (1997).
[2] N. V. Brilliantov and T. Pöschel, *Kinetic Theory of Granular Gases* (Oxford University Press, Oxford, 2004).
[3] S. Chapman and T. G. Cowling, *The Mathematical Theory of Nonuniform Gases* (Cambridge University Press, Cambridge, 1970).
[4] J. J. Brey, J. W. Dufty, C. S. Kim, and A. Santos, "Hydrodynamics for granular flow at low density," Phys. Rev. E **58**, 4638 (1998); J. J. Brey and D. Cubero, "Hydrodynamic transport coefficients of granular gases," in *Granular Gases*, Lectures Notes in Physics Vol. 564, edited by T. Pöschel and S. Luding (Springer, Berlin, 2001), p. 59.
[5] See, for instance, J. J. Brey, M. J. Ruiz-Montero, and D. Cubero, "On the validity of linear hydrodynamics for low-density granular flows described by the Boltzmann equation," Europhys. Lett. **48**, 359 (1999); J. J. Brey, M. J. Ruiz-Montero, D. Cubero, and R. García-Rojo, "Self-diffusion in freely evolving granular gases," Phys. Fluids **12**, 876 (2000); V. Garzó and J. M. Montanero, "Transport coefficients of a heated granular gas," Physica A **313**, 336 (2002); J. M. Montanero, A. Santos, and V. Garzó, "DSMC evaluation of the Navier–Stokes shear viscosity of a granular fluid," in *Rarefied Gas Dynamics 24*, AIP Conf. Proc. No. 72, edited by M. Capitelli (AIP, New York, 2005), p. 803.
[6] J. T. Jenkins and F. Mancini, "Kinetic theory for binary mixtures of smooth, nearly elastic spheres," Phys. Fluids A **1**, 2050 (1989); P. Zamankhan, "Kinetic theory for multicomponent dense mixtures of slightly inelastic spherical particles," Phys. Rev. E **52**, 4877 (1995); B. Arnarson and J. T. Willits, "Thermal diffusion in binary mixtures of smooth, nearly elastic spheres with and without gravity," Phys. Fluids **10**, 1324 (1998); J. T. Willits and B. Arnarson, "Kinetic theory of a binary mixture of nearly elastic disks," *ibid.* **11**, 3116 (1999); M. Alam, J. T. Willits, B. Arnarson, and S. Luding, "Kinetic theory of a binary mixture of nearly elastic disks with size and mass disparity," *ibid.* **14**, 4085 (2002); B. Arnarson and J. T. Jenkins, "Binary mixtures of inelastic hard spheres: Simplified constitutive theory," *ibid.* **16**, 4543 (2004).
[7] M. López de Haro, E. G. D. Cohen, and J. M. Kincaid, "The Enskog theory for multicomponent mixtures. I. Linear response theory," J. Chem. Phys. **78**, 2746 (1983).
[8] V. Garzó and J. W. Dufty, "Homogeneous cooling state for a granular mixture," Phys. Rev. E **60**, 5706 (1999).
[9] See, for instance, J. M. Montanero and V. Garzó, "Monte Carlo simulation of the homogeneous cooling state for a granular mixture," Granular Matter **4**, 17 (2002); A. Barrat and E. Trizac, "Lack of energy equipartition in homogeneous heated binary granular mixtures," *ibid.* **4**, 57 (2002); R. Clelland and C. M. Hrenya, "Simulations of a binary-sized mixture of inelastic grains in rapid shear flow," Phys. Rev. E **65**, 031301 (2002); S. R. Dahl, C. M. Hrenya, V. Garzó, and J. W. Dufty, "Kinetic temperatures for a granular mixture," *ibid.* **66**, 041301 (2002); R. Pagnani, U. M. B. Marconi, and A. Puglisi, "Driven low density granular mixtures," *ibid.* **66**, 051304 (2002); D. Paolotti, C. Cattuto, U. M. B. Marconi, and A. Puglisi, "Dynamical properties of vibrofluidized granular mixtures," Granular Matter **5**, 75 (2003); P. Krouskop and J. Talbot, "Mass and size effects in three-dimensional vibrofluidized granular mixtures," Phys. Rev. E **68**, 021304 (2003); H. Wang, G. Jin, and Y. Ma, "Simulation study on kinetic temperatures of vibrated binary granular mixtures," *ibid.* **68**, 031301 (2003); J. J. Brey, M. J. Ruiz-Montero, and F. Moreno, "Energy partition and segregation for an intruder in a vibrated granular system under gravity," Phys. Rev. Lett. **95**, 098001 (2005).
[10] R. D. Wildman and D. J. Parker, "Coexistence of two granular temperatures in binary vibrofluidized beds," Phys. Rev. Lett. **88**, 064301 (2002); K. Feitosa and N. Menon, "Breakdown of energy equipartition in a 2D binary vibrated granular gas," *ibid.* **88**, 198301 (2002).
[11] J. Jenkins and F. Mancini, "Balance laws and constitutive relations for plane flows of a dense binary mixture of smooth, nearly elastic, circular disks," J. Appl. Mech. **54**, 27 (1987).
[12] V. Garzó and J. W. Dufty, "Hydrodynamics for a granular binary mixture at low density," Phys. Fluids **14**, 1476 (2002).
[13] J. M. Montanero and V. Garzó, "Shear viscosity for a heated granular binary mixture at low-density," Phys. Rev. E **67**, 021308 (2003).
[14] V. Garzó and J. M. Montanero, "Diffusion of impurities in a granular gas," Phys. Rev. E **69**, 021301 (2004).
[15] S. R. Dahl, C. M. Hrenya, V. Garzó, and J. W. Dufty, "Kinetic temperatures for a granular mixture," Phys. Rev. E **66**, 041301 (2002).
[16] L. Huilin, D. Gidaspow, and E. Manger, "Kinetic theory of fluidized binary granular mixtures," Phys. Rev. E **64**, 061301 (2001); M. F. Ramahan, J. Naser, and P. J. Witt, "An unequal temperature kinetic theory: description of granular flow with multiple particle classes," Powder Technol. **138**, 82 (2003); J. E. Galvin, S. R. Dahl, and C. M. Hrenya, "On the influence of the equipartition-of-energy assumption in kinetic theories for rapidly-flowing, granular mixtures," J. Fluid Mech. **528**, 207 (2005).
[17] A. Santos, V. Garzó, and J. Dufty, "Inherent rheology of a granular fluid in uniform shear flow," Phys. Rev. E **69**, 061303 (2004).
[18] J. J. Brey, M. J. Ruiz-Montero, and D. Cubero, "On the validity of linear hydrodynamics for low-density granular flows described by the Boltzmann equation," Europhys. Lett. **48**, 359 (1999).
[19] J. J. Brey, M. J. Ruiz-Montero, F. Moreno, and R. García-Rojo, "Transversal inhomogeneities in dilute vibrofluidized granular fluids," Phys. Rev. E **65**, 061302 (2002); J. J. Brey, M. J. Ruiz-Montero, and F. Moreno, "Hydrodynamics of an open vibrated granular system," *ibid.* **63**, 061305 (2001).
[20] X. Yang, C. Huan, D. Candela, R. W. Mair, and R. L. Walsworth, "Measurements of grain motion in a dense, three-dimensional granular fluid," Phys. Rev. Lett. **88**, 044301 (2002); C. Huan, X. Yang, D. Candela, R. W. Mair, and R. L. Walsworth, "NMR experiments on a three-dimensional vibrofluidized granular medium," Phys. Rev. E **69**, 041302 (2004).
[21] C. Bizon, M. D. Shattuck, J. B. Swift, and H. L. Swinney, "Transport coefficients for granular media from molecular dynamics simulations," Phys. Rev. E **60**, 4340 (1999); E. C. Rericha, C. Bizon, M. D. Shattuck, and H. L. Swinney, "Shocks in supersonic sand," Phys. Rev. Lett. **88**, 014302 (2002).
[22] S. R. de Groot and P. Mazur, *Nonequilibrium Thermodynamics* (Dover, New York, 1984).
[23] Note that this coefficient is not strictly zero in the approximation used here due to the fact that while the set $\{d_i'', \ell_i, \lambda_i\}$ has been evaluated in the second Sonine approximation, the coefficients D^*, D_p^*, and D'^* have been estimated in the first Sonine approximation. However, the magnitude of L_p is negligible.
[24] A. Santos and J. W. Dufty, "Critical behavior of a heavy particle in a granular fluid," Phys. Rev. Lett. **86**, 4823 (2001); "Nonequilibrium phase transition for a heavy particle in a granular fluid," Phys. Rev. E **64**, 051305 (2001).
[25] V. Garzó, "Instabilities in a free granular fluid described by the Enskog equation," Phys. Rev. E **72**, 021106 (2005).
[26] V. Garzó and J. W. Dufty, "Dense fluid transport for inelastic hard spheres," Phys. Rev. E **59**, 5895 (1999).
[27] Some misprints occur in the expressions given in Ref. 12 for these quantities. The expressions given here correct such results.
[28] See Ref. 3, Chap. 9, Eqs. (9.6,1)–(9.6,10).